Microelectronic Engineering 86 (2009) 88–95

Contents lists available at ScienceDirect

Microelectronic Engineering

journal homepage: www.elsevier.com/locate/mee

Barrier characteristics of gold Schottky contacts on moderately doped n-InP based on temperature dependent *I–V* and *C–V* measurements

M. Soylu, B. Abay *

Atatürk Üniversitesi, Fen-Edebiyat Fakültesi, Fizik Bölümü, 25240 Erzurum, Turkey

ARTICLE INFO

Article history:
Received 27 June 2008
Received in revised form 20 September 2008
Accepted 28 September 2008
Available online 18 October 2008

PACS:
73.30.+y
73.40.Qv
73.40.Ns

Keywords:
InP
Schottky diode
Temperature dependent *I–V* and *C–V* measurements
Gaussian distribution
Barrier inhomogeneities

ABSTRACT

The temperature dependences of current–voltage (*I–V*) and capacitance–voltage (*C–V*) characteristics of the gold Schottky contacts on moderately doped n-InP (Au/MD n-InP) Schottky barrier diodes (SBDs) have been systematically investigated in the temperature range of 60–300 K. The main diode parameters, ideality factor (n) and zero-bias barrier height (apparent barrier height) (Φ^{j}_{b0}) were found to be strongly temperature dependent and while the Φ^{j}_{b0} decreases, the n and the (Φ^{C}_{b}) increase with decreasing temperature. According to Thermionic Emission (*TE*) theory, the slope of the conventional Richardson plot [$In(J_0/T^2)$ vs. $1000/T$] should give the barrier height. However, the experimental data obtained do not correlate well with a straight line below 160 K. This behaviour has been interpreted on the basis of standard *TE* theory and the assumption of a Gaussian distribution of the barrier heights due to barrier inhomogeneities that persist at the metal-semiconductor interface. The linearity of the apparent barrier height (Φ^{j}_{b0}) vs. $1/(2kT)$ plot that yields a mean barrier height ($\overline{\Phi}^{j}_{b0}$) of 0.526 eV and a standard deviation (σ_{s0}) of 0.06 eV, was interpreted as an evidence to apply the Gaussian distribution of the barrier height. Furthermore, modified Richardson plot [$In(J_0/T^2) - (q^2\sigma^2_{s0}/2\,k^2T^2)$ vs. $1/T$] has a good linearity over the investigated temperature range and gives the $\overline{\Phi}^{j}_{b0}$ and the Richardson constant (A^*) values as 0.532 eV and 15.90 $AK^{-2}cm^{-2}$, respectively. The mean barrier heights obtained from both plots are appropriate with each other and the value of A^* obtained from the modified Richardson plot is close to the theoretical value of 9.4 $AK^{-2}cm^{-2}$ for n-InP. From the *C–V* characteristics, measured at 1 MHz, the capacitance was determined to increase with increasing temperature. *C–V* measurements have resulted in higher barrier heights than those obtained from *I–V* measurements. The discrepancy between Schottky barrier heights (SBHs) obtained from *I–V* and *C–V* measurements was also interpreted. As a result, it can be concluded that the temperature dependent characteristic parameters for Au/MD n-InP SBDs can be successfully explained on the basis of *TE* mechanism with Gaussian distribution of the barrier heights.

1. Introduction

The metal-semiconductor (MS) structures are of important applications in the electronics industry. These applications consist of microwave field effect transistors, radio-frequency detectors, phototransistors, heterojunction bipolar transistors, quantum confinement devices and space solar cell [1–3]. The performance and reliability of a Schottky contact is highly influenced by the interface quality between the deposited metal and the semiconductor surface. In order to understand the conduction mechanism of the Schottky barrier diodes (SBDs), many attempts have been made. Generally, the SBD parameters are determined over a wide range of temperatures and doping concentrations in order to understand the nature of the barrier and the conduction mechanism.

The analysis of the current–voltage (*I–V*) characteristics of Schottky barriers on the basis of thermionic emission diffusion (*TED*) theory reveals an abnormal decrease of the barrier height (BH) and increase of the ideality factor with decreasing temperature [1–4]. Also, the ideality factor has been found to increase with increasing carrier concentration, while BH obtained by the *I–V* measurements decreases with increasing doping level [1]. Explanation of the possible origin of such anomalies have been proposed by taking into account the interface state density distribution [5], quantum-mechanical tunnelling [1,6,7], image-force lowering [1] and most recently the lateral distribution of BH inhomogeneities [2,8,9]. In addition, a Gaussian distribution of the BH over the contact area has been assumed to describe the inhomogeneities as an other way too [2,10].

Indium Phosphide (InP) being one of the III–V compound semiconductors is a promising material for high-speed electrical and optoelectronic devices due to its large direct band gap, high electron mobility, high saturation velocity and breakdown voltage

* Corresponding author. Tel.: +00 90 442 231 41 81; fax: +00 90 442 236 09 48.
E-mail address: babay@atauni.edu.tr (B. Abay).

0167-9317/$ - see front matter © 2008 Elsevier B.V. All rights reserved.
doi:10.1016/j.mee.2008.09.045

which are very important in electronic devices [11,12]. But, due to the large reverse leakage current for metal/n-InP structures it is difficult to obtain a Schottky barrier height (SBH) greater than 0.5 eV [1,12–18]. Thus, the use of n-InP has been hindered in this area. However, low BH Schottky diodes of n-InP seem to be a good candidate for the application of zero-bias Schottky detector diodes [12].

Newman et al. [14] have studied the electrical transport characteristics of nine metals on n-GaAs and n-InP as a function of doping level on (1 1 0) surfaces. Furthermore, Horváth et al. [15] have presented experimental results obtained on n-type InP using various Schottky metal on untreated and/or HF, HF + Na_2S and HCl treated surface. Most of studies have been done on n-InP wafers with unintentionally doped or with low doping level [11–18].

In this study, the current–voltage (*I–V*) and capacitance–voltage (*C–V*) measurements of the gold Schottky contacts on moderately doped n-InP (Au/MD n-InP) SBDs have been made over the temperature range of 60–300 K. The resultant temperature dependent barrier characteristics of the diodes have been interpreted on the basis of the existence of Gaussian distribution of the barrier height.

2. Experimental details

SBDs were fabricated on moderately S-doped n-type InP (100) substrate with doping agent concentration of 1.2×10^{16} cm^{-3}. The substrate was sequentially cleaned with trichloroethylene, acetone, and methanol and then rinsed in deionised water. The native oxide on the surface was etched in sequence with acid solutions (H_2SO_4:H_2O_2:H_2O = 3:1:1) for 60 seconds, and (HF (49%):H_2O = 1:1) for another 60 s. After a rinse in deionised water a blow-dry with nitrogen. Low resistance Ohmic contact on the back side of the sample was formed by evaporating of Au:Ge eutectic alloy (88% Au:12% Ge) at a pressure of 2×10^{-6} mbar, followed by annealing at 300 °C for 5 min in nitrogen atmosphere. Then, the above procedures were also used to clean the front surface. Finally, circular dots with a diameter of approximately 1 mm of Au were then evaporated through a molybdenum mask at a pressure of 2×10^{-6} mbar to form the Schottky barriers.

I–V and *C–V* measurements of the devices were made using a computer controlled Keithley 487 picoammeter/voltage source and an HP 4192 A LF impedance analyser, respectively over the temperature range of 60–300 K and in dark. The measurements below room temperature were performed by mounting the device onto the specially designed cold finger of ARS HC-2 closed-cycle helium cryostat. The device temperature was controlled within an accuracy of ±0.1 K by a Lake Shore 331 model temperature controller.

3. Results and discussion

3.1. The current–voltage characteristics as function of temperature

The current density (*J*) through a SBD at a forward bias (*V*), according to thermionic emission (*TE*) theory, is given by [19,20]

$$J = J_0 \exp\left(\frac{qV_d}{nkT}\right)\left[1 - \exp\left(-\frac{qV_d}{kT}\right)\right] \quad (1)$$

where $V_d = (V - IR_s)$ is the diode voltage, J_0 is the reverse saturation current density derived from the straight line intercept of $In(J)$ at zero-bias and is given by

$$J_0 = A^* T^2 \exp\left(-\frac{q\Phi_{b0}^j}{kT}\right). \quad (2)$$

Where q is the electronic charge, V is the definite forward bias voltage, A^* is the effective Richardson constant, k is the Boltzmann constant, T is the absolute temperature, Φ_{b0}^j is the zero-bias current-barrier height (apparent barrier height) and n is the ideality factor. From Eq. (1), the ideality factor n can be written as

$$n = \frac{q}{kT}\left(\frac{dV}{dIn(J)}\right). \quad (3)$$

Fig. 1 shows forward bias semi-logarithmic $J - V$ characteristics of an Au/MD n-InP SBD in the temperature range of 60–300 K. The values of Φ_{b0}^j and n determined from the intercept and the slopes of the forward bias $In(J)$ versus voltage (V) plot according to *TE* theory are shown in Figs. 2 and 3 as a function of temperature, respectively. Richardson constant of electrons in n-type InP was calculated as $A^* = 120 m_e^*/m_0 = 9.4$ $AK^{-2}cm^{-2}$, where $m_e^*(= 0.078 m_0)$ is the effective mass for electrons [21]. The experimental values of the Φ_{b0}^j and n range from 0.194 eV and 2.895 at 60 K to 0.465 eV and 1.029 at 300 K, respectively. The values of the Φ_{b0}^j are the effective values and do not take into account the image-force lowering. This value is comparable with those of obtained by Szydlo and Oliver [22] and Benamara et al. [23], which are equal to about 0.46 eV, 0.441 eV, respectively and that found by Shi et al. [24], which is 0.51 eV, for Au/n-InP contacts. The series resistance R_S varies between 3 and 5 Ω, and is almost independent of temperature. As seen in Figs. 2 and 3, both of the n and Φ_{b0}^j are strongly dependent on temperature and the changes are more pronounced below 160 K. Such a behaviour of the ideality factor has been attributed to the particular distribution of the interface states. Since current transport across the metal-semiconductor interface is controlled by temperature, electrons at low temperature pass over the lower barriers and therefore current will flow through patches of the lower SBH and results in a larger ideality factor. In other words, more electrons have sufficient energy to overcome the higher barrier.

To determine the BH in another way, the Richardson plot is drawn. Eq. (2) can be rewritten as

$$In\left(\frac{J_0}{T^2}\right) = InA^* - \frac{q\Phi_{b0}^j}{kT}. \quad (4)$$

Fig. 4 shows the conventional Richardson plot. The experimental data show a bowing at low temperature and it appears a straight line above 160 K. Φ_{b0}^j obtained from the slope of this straight line yields to be 0.30 eV. Similarly, the value of A^* obtained from the intercept at the ordinate is equal to 1.70×10^{-2} $AK^{-2}cm^{-2}$, which is lower than the known value of 9.4 $AK^{-2}cm^{-2}$

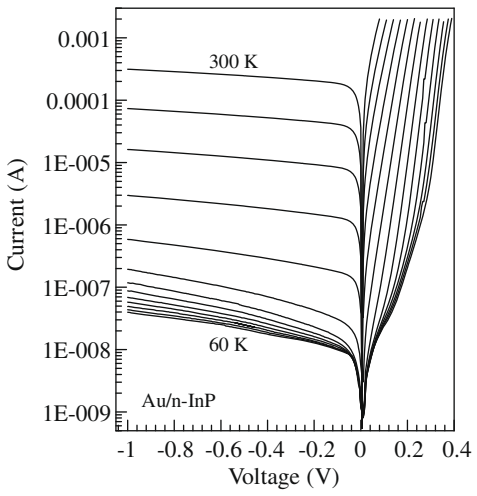

Fig. 1. Semi-logarithmic reverse and forward bias current–voltage characteristics of an Au/MD n-InP Schottky barrier diode at various temperatures.

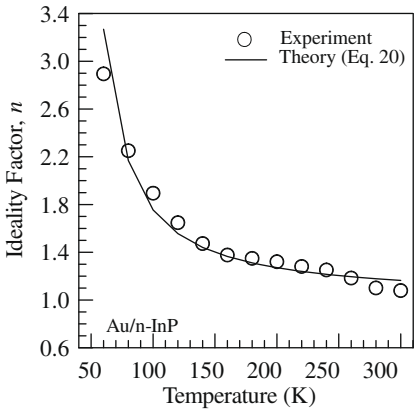

Fig. 2. Temperature dependence of the ideality factor of the Au/MD n-InP Schottky barrier diode in the temperature range of 60–300 K. The continuous curve shows the estimated value of the ideality factor using Eq. (20) with $\rho_2 = -4.032 \times 10^{-3}$ and $\rho_3 = -7.485 \times 10^{-3}$ eV.

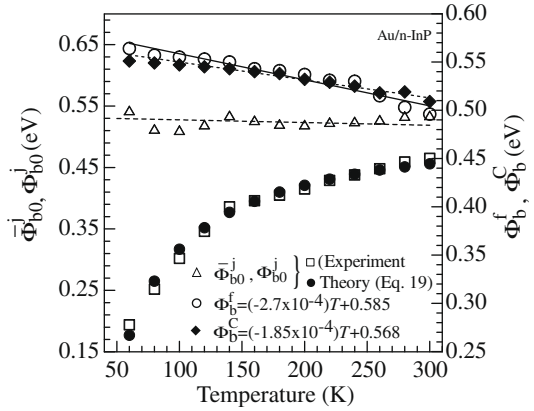

Fig. 3. Temperature dependence of the zero-bias BH (Φ^{j}_{b0}), mean BH ($\bar{\Phi}^{j}_{b0}$), flat-band BH (Φ^{f}_{b}) and capacitance BH (Ψ^{c}_{b}) for the Au/MD n-InP Schottky barrier diode in the temperature range of 60–300 K. The closed circles represent the estimated value of Φ^{j}_{b0} using Eq. (19) with $\bar{\Phi}^{j}_{b0}$ and σ_{s0} 0.526 eV and 0.060 eV, respectively.

for n-InP. The bowing in the Richardson plots may be due to the spatial inhomogeneous barrier heights and potential fluctuations at the interface that consist of low and high barrier areas [2,25–31]. As will be discussed below, the deviation in the Richardson plots can be explained by assuming the effects of the image-force, the effect of tunnelling current through the potential barrier, the effect of recombination in the space charge region appearing at low voltage and the variation of the charge distribution near the interface [32].

3.1.1. Effect of image-force lowering

BH lowering and the increase in ideality factor with decreasing measurement temperature can be considered to be due to the image-force lowering at first sight and its relation is given by [19,20]

$$\Delta\Phi_{imf} = \left\{ \left(\frac{q^3 N_d}{8\pi^2 \varepsilon_s^3} \right) \left[\Phi^{j}_{b0} - V - \xi - \frac{kT}{q} \right] \right\}^{1/4} \tag{5}$$

where $\xi = \frac{kT}{q} \ln(N_c/N_d)$, V is the applied bias voltage, N_c (=1.052 $\times 10^{14} T^{3/2}$ cm^{-3}) is the effective conduction band density of the states [21], N_d (=1.12 $\times 10^{16}$ cm^{-3} and 8.34 $\times 10^{15}$ cm^{-3} for T = 300 K and 60 K, respectively) is the ionized donor density of the n-InP obtained by temperature dependent C–V measurement and ε_s (=12.4ε_0) is the permittivity of InP [21]. The values of $\Delta\Phi_{imf}$ found by using Eq. (5) are 19.7 and 15.6 meV at 300 and 60 K,

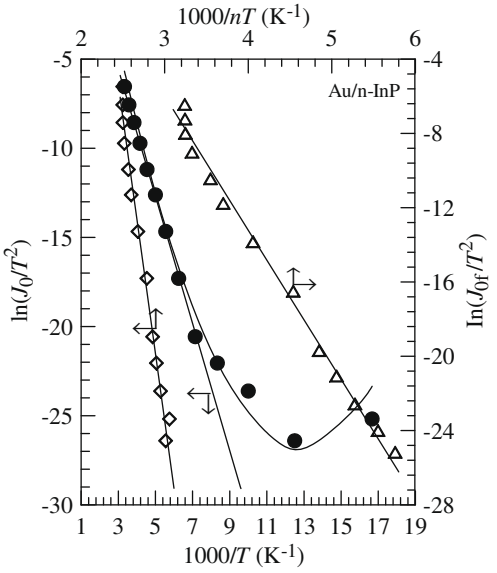

Fig. 4. Richardson plots of $\ln(J_0/T^2)$ vs. 1000/T or 1000/nT and $\ln(J_{0f}/T^2)$ vs. 1000/nT and their linear fits for the Au/MD n-InP Schottky diode. The continuous curve represents the data obtained by using Eqs. (18) and (19) with the parameters $\bar{\Phi}^{j}_{b0}$ = 0.526 eV, σ_0 = 0.060 eV and A^* = 15.9 AK^{-2}cm^{-2}.

respectively. These values of $\Delta\Phi_{imf}$ point out that the influence of the barrier lowering due to the image-force on the Φ^{j}_{b0} are nearly constant in the investigated temperature region and the image-force effect alone cannot account for the decreasing of the barrier height with decreasing temperature.

Also, the increase in the ideality factor with decreasing measurement temperature might be due to the image-force lowering; then, the following relation can be used for interpreting the values of the ideality factors calculated [20,33]:

$$\frac{1}{n_{imf}} = 1 - \frac{1}{4} \left(\frac{q^3 N_d}{8\pi^2 \varepsilon_s^3} \right)^{1/4} \left[\Phi^{j}_{b0} - V - \xi - \frac{kT}{q} \right]^{-3/4}. \tag{6}$$

The ideality factors found by using Eq. (6) are 1.015 and 1.022 at 300 and 60 K, respectively. These values also show that the observed variation in the ideality factor cannot be explained by the image-force lowering. In this case, the other current transport mechanisms such as Thermionic Field Emission (*TFE*) or recombination generation should be accounted as the reason of the increase in the ideality factor with decreasing measurement temperature [20,33].

3.1.2. Effect of thermionic field emission

The decrease in the BH and the increase in the ideality factor with a decrease in the measurement temperature are indicatives of a derivation from the pure *TE* theory and possibly the *TFE* mechanism warrants consideration. If current transport is controlled by *TFE* theory, the connection between the current density and voltage can be expressed by [20]

$$J = J_0 \exp\left(\frac{V}{E_0}\right) \tag{7}$$

$$E_0 = E_{00} \coth\left(\frac{E_{00}}{kT}\right) \tag{8}$$

$$E_{00} = \frac{q\hbar}{2} \left(\frac{N_d}{m^*_e \varepsilon_s} \right)^{1/2} \tag{9}$$

where E_{00} is the characteristic energy, which is related to the transmission probability, N_d (=1.12 $\times 10^{16}$ cm^{-3} and 8.34 $\times 10^{15}$ cm^{-3} for T = 300 K and 60 K, respectively) is the ionized donor density

of n-InP obtained from the temperature dependent capacitance measurement, $m_e^* = 0.078\ m_0$ [21], and $\varepsilon_s = 12.4\varepsilon_0$ [21] for InP. The values of E_{00} have been evaluated as 2.02 and 1.73 meV for $T = 300$ K and 60 K, respectively. To see the effect of free carriers and to define the dominant current mechanism of the Schottky contact, E_{00} values have been normalized to kT in the investigated temperature region. As seen in Fig. 5, normalized E_{00}/kT values decreases with temperature and $E_{00} \ll kT$ condition is satisfied for the investigated temperature range. According to the theory, field emission (*FE*) becomes important when $E_{00} \gg kT$ whereas, *TFE* dominates when $E_{00} \approx kT$ and *TE* is crucial if $E_{00} \ll kT$. Therefore, we can postulate that all over the temperature range *TE* is the dominant current mechanism.

In addition, the ideality factor n is related to the E_{00} as [20]:

$$n_{tun} = \frac{qE_{00}}{kT}\coth\left(\frac{qE_{00}}{kT}\right). \tag{10}$$

According to the Eq. (10) the contribution of *TFE* results only in an increase of 1.049 for n at 60 K. This value is too low to explain our measured value ($n = 2.895$) at 60 K. As a result, the possibility of the *FE* and *TFE* can be ruled out. Thus, the higher n values may be related to *TE* over a Gaussian barrier height distribution and it will be discussed below.

Furthermore, using Eq. (10) in our previous study [34], experimental temperature dependent values of the ideality factor obtained from the experimental *I–V* characteristics in Fig. 1 is in agreement with $E_{00} = 16.0$ meV in the investigated temperature region without considering the bias coefficient of the barrier height, $\beta = 0$. This value of the characteristic energy E_{00} is about eight times larger than the value of 2.02 meV calculated for the n-InP. Such a difference between the theoretical and experimental data is usually obtained and expected for Schottky diodes and this case is connected with local enhancement of electrical field which can also yield a local reduction of the BH [35].

3.1.3. Flat-band barrier height and modified Richardson plots

The barrier height obtained under flat-band condition is called the flat-band barrier height and it is considered as the real fundamental quantity. It should be used when comparing experiments with theory. In this case, the electric field in the semiconductor is zero and thus the semiconductor bands are flat, but the case of zero-bias barrier height is not valid. The influence of lateral inhomogeneities on the evolution of the current–voltage characteristics is eliminated by using the flat-band barrier height Φ_b^f instead of the zero-bias barrier height Φ_{b0}^j. The flat-band barrier height is given by [25,36,37]

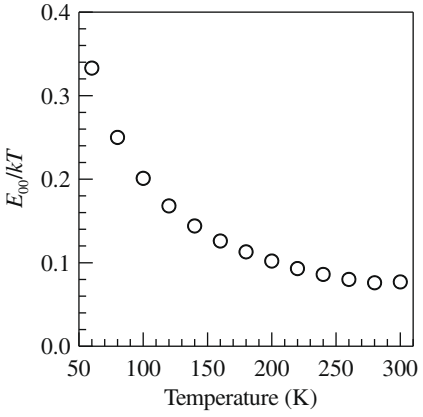

Fig. 5. Normalized E_{00}/kT values as a function of temperature.

$$\Phi_b^f = n\Phi_{b0}^j - (n-1)\left(\frac{kT}{q}\right)\ln\left(\frac{N_c}{N_d}\right) \tag{11}$$

where N_c is the effective density of states in the conduction band.

A plot of the flat-band barrier height Φ_b^f as a function of temperature is also displayed in Fig. 3 (indicated by open circles). As seen in this figure, Φ_b^f is always larger than Φ_{b0}^j and, unlike Φ_{b0}^j, it increases with decreasing temperature. The temperature dependence of the flat-band barrier height can be expressed as [25]

$$\Phi_b^f(T) = \Phi_b^f(T=0) - \alpha T. \tag{12}$$

Where $\Phi_b^f(T=0)$ and α are the flat-band barrier height extrapolated to the absolute zero and the temperature coefficient of the flat-band barrier height, respectively. In the Fig. 3, the fitting of the $\Phi_b^f(T)$ data to Eq. (12) yields $\Phi_b^f(T=0) = 0.585$ eV and $\alpha = -2.7 \times 10^{-4}$ eVK^{-1} in the temperature range 60–300 K. Using Φ_b^f instead of Φ_{b0}^j, flat-band saturation current density J_{0f} can be written similar to the Eq. (2) as [13,38]

$$J_{0f} = A^*T^2\exp\left(-\frac{q\Phi_b^f}{nkT}\right). \tag{13}$$

So, the relation between J_{0f} and zero-bias saturation current density J_0 is given by

$$J_{0f} = J_0\exp\left[\left(\frac{n-1}{n}\right)\ln\left(\frac{N_c}{N_d}\right)\right]. \tag{14}$$

When considering the ideality factor varies with temperature, the plot of $ln(J_{0f}/T^2)$ versus $1000/nT$ according to Eq. (13) should be a straight line with the slope and the intercept at the ordinate, directly yielding Φ_b^f and A^*, respectively. The $ln(J_{0f}/T^2)$ versus $1000/nT$ plot is also shown in the Fig. 4 as open triangles. The linear portion of this plot gives 0.622 eV and 25.34 A cm^{-2}K^{-2} for $\Phi_b^f(T=0)$ and $A^*_{corr.}$ considering $A^*_{corr} = A^*\exp(q\alpha/k)$ [29,39], respectively. These results show that the value of the Richardson constant is different from the known theoretical value of 9.4 AK^{-2}cm^{-2} for electrons in the n-type InP.

3.1.4. The analysis of barrier height inhomogeneities

The ideality factor is simply a manifestation of the barrier uniformity [40]. A significant increase in the ideality factor and decrease in the SBH at low temperature are possibly originated by structural defects in the semiconductor, inhomogeneous doping, interface roughness, interfacial reactions, diffusion/interdiffusion of the contaminations of applied materials on semiconductor surface, inhomogeneities of thickness and composition of the layer, and non-uniformity of interfacial charges or the presence of a thin insulating layer between the metal and the semiconductor [3,25,26,40–42]. Since current transport across the MS interface is a temperature-activated process, the current will be controlled by the current through the patches having low BH at the low temperatures. Werner and Güttler [3,25] have proposed an analytical potential fluctuation model for the interpretation of *I–V* and *C–V* measurements on spatially inhomogeneous PtSi/*Si* Schottky contacts, while Henisch [43] speculated that the fluctuations in BHs are unavoidable as they exist even in the most carefully processed devices. Furthermore, a linear correlation between the experimental zero-bias BH Φ_{b0}^j and the ideality factor n has been obtained utilizing Tung's pinch-off model [5] by Schmitsdorf et al. [9,44]. Fig. 6 shows an example of this plot for Au/MD n-InP SBD. A linear relationship between the Φ_{b0}^j and n values in Fig. 6 is an indication of the barrier irregularity and can be explained by lateral inhomogeneities of the BHs [44]. A homogeneous BH of approximately 0.466 eV obtained from the extrapolation of the least-square linear fitting to data to $n = 1$ (Fig. 6) is in agreement with the values obtained by Anand et al. [45], Brillson et al. [16], Hökelek and

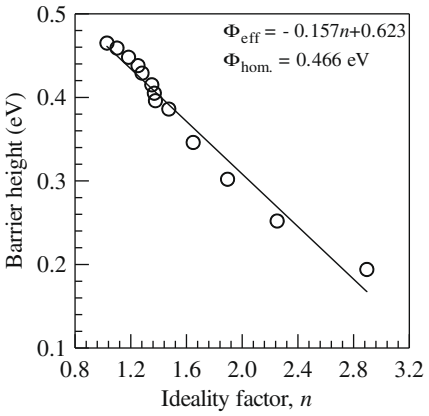

Fig. 6. Plot of the zero-bias BH Φ^{j}_{b0} versus ideality factor (n) at the investigated temperature range.

Robinson [17] and Çetin et al. [18] on the Au/n-InP and Horváth et al. [12] on the Au–Cr/n-InP SBDs.

In order to describe the abnormal behaviours mentioned above, an analytical potential fluctuation model using different types of barrier distribution function at the interface on the spatially inhomogeneous SBDs has been proposed by different workers [3,10,25–27,30,31,40–42,46]. A spatial distribution of the barrier height at the metal-semiconductor interface of Schottky contacts by a Gaussian distribution $P(\Phi^{j}_{b})$ with a standard deviation (σ_s) around a mean SBH (Φ^{j}_{b}) value has been suggested by Werner and Güttler [3,25] as:

$$P(\Phi^{j}_{b}) = \frac{1}{\sigma_s\sqrt{2\pi}} \exp\left[-\frac{(\Phi^{j}_{b} - \overline{\Phi}^{j}_{b})^2}{2\sigma_s^2}\right], \tag{15}$$

where $1/\sigma_s\sqrt{2\pi}$ stands for the normalizing constant. Hence, the net current density for any forward bias V is then given by

$$J(V) = A^{*}T^{2} \times \exp\left[-\frac{q}{kT}\left(\overline{\Phi}^{j}_{b} - \frac{q\sigma_s^2}{2kT}\right)\right] \exp\left(\frac{qV_d}{kT}\right)\left[1 - \exp\left(-\frac{qV_d}{kT}\right)\right]. \tag{16}$$

Since the BH is known to depend on the electric field and hence on the applied voltage, the entire profile is also affected by the bias. By assuming a linear bias dependence of both the mean barrier height $\overline{\Phi}^{j}_{b}$ and square of the standard deviation σ_s^2 with coefficients ρ_2 and ρ_3, (i.e., $\overline{\Phi}^{j}_{b}(V) = \overline{\Phi}^{j}_{b0} + \rho_2 V$ and $\sigma_s^2(V) = \sigma_{s0}^2 + \rho_3 V$), respectively, Eq. (16) gets modified as:

$$J = J_0 \exp\left(\frac{qV_d}{n_{ap}kT}\right)\left[1 - \exp\left(-\frac{qV_d}{kT}\right)\right] \tag{17}$$

with

$$J_0 = A^{*}T^{2} \exp\left(-\frac{q\Phi_{ap}}{kT}\right). \tag{18}$$

Where Φ_{ap} and n_{ap} are called as apparent zero-bias barrier height and apparent ideality factor, respectively, and are given by [3]

$$\Phi_{ap} = \overline{\Phi}^{j}_{b0} - \frac{q\sigma_{s0}^2}{2kT} \tag{19}$$

$$1/n_{ap}(T) - 1 = -\rho_1(T) = -\rho_2 + \frac{q\rho_3}{2kT} \tag{20}$$

where ρ_1, ρ_2 and ρ_3 are the voltage coefficients and depict the voltage deformation of the barrier height distribution, while $\overline{\Phi}^{j}_{b0}$ and σ_{s0} are the mean barrier height and its standard deviation at the zero-bias ($V = 0$), respectively. Since the Φ_{ap} depends on the distribution parameters $\overline{\Phi}^{j}_{b0}$ and σ_{s0}, and temperature, the decrease of the apparent zero-bias BH is affected by the existence of the interface inhomogeneities and this effect becomes more significant at low temperatures. On the other hand, the abnormal increase in n_{ap} comes up mainly due to the bias coefficients (ρ_2 and ρ_3) of the mean barrier height and the standard deviation. Whilst ρ_2 gives a constant shift, ρ_3 causes its temperature dependent variation and gets into significance at low temperature.

As Eqs. (2) and (18) are of the same form, the fitting of the experimental J–V data to Eq. (16) gives Φ_{ap} and n_{ap}, which should obey Eqs. (19) and (20). Thus, the plot of Φ_{ap} vs. l/2kT (Fig. 7) should be a straight line yielding $\overline{\Phi}^{j}_{b0}$ and σ_{s0} from the intercept and slope, respectively. The values of 0.526 eV and 0.060 eV for $\overline{\Phi}^{j}_{b0}$ and σ_{s0}, respectively were obtained from the least-square linear fitting of the data. Furthermore, as can be seen from Fig. 3, the experimental results of Φ_{ap} (denoted by open squares) fit very well with Eq. (19) (denoted by closed circles) with the same parameters. Also, the correction to the experimental data has been made using Eq. (19). The values of $\overline{\Phi}^{j}_{b0}$ are marked as zero-bias mean barrier height (denoted by open triangles) in Fig. 3. When comparing $\overline{\Phi}^{j}_{b0}$ and σ_{s0} parameters, it is seen that the standard deviation is ≈10% of the mean zero-bias barrier height. The standard deviation is a measure of the barrier homogeneity. The lower value of σ_{s0} corresponds to a more homogeneous barrier height. It is seen that the value of σ_{s0} = 0.060 eV is not small compared to the mean value of $\overline{\Phi}^{j}_{b0}$ = 0.526 eV and it indicates larger inhomogeneities at the interface of our Au/MD n-InP Schottky structure. Hence, this inhomogeneity and potential fluctuation dramatically affect low temperature I–V characteristics and it is responsible, in particular, for the curved behaviour in the conventional Richardson plot denoted by closed circles in Fig. 4.

Fig. 7 also shows the $(1/n_{ap} - 1)$ vs. $1/2kT$ plot. According to Eq. (20), this plot should be a straight line that gives the voltage coefficients ρ_2 and ρ_3 from the intercept and slope, respectively. The values of $\rho_2 = -4.03 \times 10^{-3}$ and $\rho_3 = -7.49 \times 10^{-3}$ eV have been obtained from this plot. Furthermore, the experimental results of n in Fig. 2 can be seen to fit very well with Eq. (20), denoted by solid line, with the same parameters. The linear behaviour of $(1/n_{ap} - 1)$ vs. $1/2kT$ plot confirms that the ideality factor does indeed denote the voltage deformation of the Gaussian distribution of the BH. It is clear from the Eq. (20) that when becomes ρ_3 negative, it will be responsible for the increase in n_{ap} with a decrease in temperature. As ρ_2 becomes also negative, we can also conclude that the barrier height and its standard deviation are decreased as bias increases. These results reveal that a bias voltage obviously homogenizes the BH fluctuation, i.e., the higher the bias, the

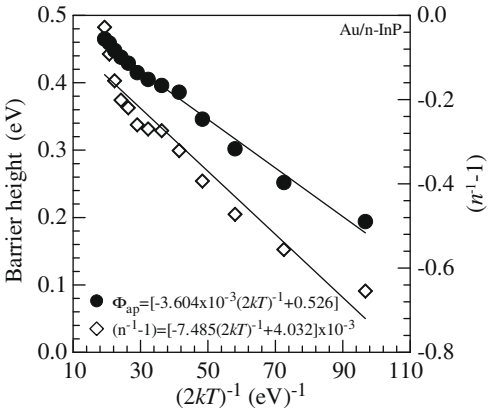

Fig. 7. Zero-bias BH Φ^{j}_{b0} and $(1/n_{ap} - 1)$ vs. $1/2kT$ plots and their linear fits for the Au/MD n-InP Schottky diode according to Gaussian distribution of the barrier heights.

narrower the BH distribution, which can be explained that image-forces shift the effective barrier maximum deeper into the semiconductor when the bias voltage increases. Thus, homogenizing the BH distribution [29].

Since the conventional Richardson plot deviates from linearity at low temperatures due to the barrier inhomogeneity, it can be modified by combining Eqs. (18) and (19) as follows:

$$In\left(\frac{J_0}{T^2}\right)-\left(\frac{q^2\sigma_{s0}^2}{2k^2T^2}\right)=InA^*-\frac{q\overline{\Phi}_{b0}^{j}}{kT}. \tag{21}$$

Hence, modified Richardson plot $[\ln(J_0/T^2)-(q^2\sigma_{s0}^2/2k^2T^2)$ vs.1000/T] according to Eq.(21) should also be a straight line with the slope and the intercept at the ordinate directly yielding the zero-bias mean barrier height $\overline{\Phi}_{b0}^{j}$ and A^*, respectively.As can be seen from Fig.8, the modified Richardson plot has a quite good linearity over the whole temperature range corresponding to a single activation energy around $\overline{\Phi}_{b0}^{j}$. By the least-square linear fitting of the data, $\overline{\Phi}_{b0}^{j}=0.532$ eV and $A^*=15.9$ AK^{-2}cm^{-2} are obtained. Meanwhile, this value of $\overline{\Phi}_{b0}^{j}=0.532$ eV is approximately the same as the value of $\overline{\Phi}_{b0}^{j}=0.526$ eV from the plot of Φ_{ap} vs.1/2kT given in Fig.7, while modified Richardson constant $A^*=15.9$ AK^{-2}cm^{-2} is in close agreement with the theoretical value of $A^*=9.4$ AK^{-2} cm^{-2}.Furthermore, the recreated conventional Richardson plot by using Eqs.(18) and (19) (denoted by solid curve) with the parameters $\overline{\Phi}_{b0}^{j}=0.526$ eV,$\sigma_{s0}=0.060$ eV and $A^*=15.9$ AK^{-2}cm^{-2} well correlate with the experimental points denoted by closed circles as shown in Fig. 4. These results show that the temperature dependent I–V characteristics of Au/MD n-InP Schottky structure obey the Gaussian distribution of BHs as in the case of Al/p-InP SBD [26], Ti/p-InP [34] and Pd/n-InP [47]. So, we can speculate that the lateral SB inhomogeneities are not only peculiar to the gold contacts on InP, but also other contact metals.

3.2. Capacitance–voltage characteristics as function of temperature

In a capacitance–voltage (C–V) measurement carried out at sufficiently high frequency, the charge at the interface states cannot follow the a.c. signal. This will occur when the time constant is too long to permit the charge to move in and out of the states in response to an applied signal. Thus, for a SBD fabricated on an n-type semiconductor, the depletion layer capacitance can be expressed as [48]

$$\frac{1}{C^2}=\frac{2(V_{bi}+V_r-kT/q)}{q\varepsilon_s\varepsilon_o A^2N_i}, \tag{22}$$

where V_{bi} is the built-in voltage determined from the extrapolation of the $C^{-2}-V$ plot to the voltage axis, V_r is the reverse voltage, A is the area of the diode, ε_s is the static dielectric constant equal to 12.4 for n-InP [21], $\varepsilon_o=8.85\times10^{-14}$ F/cm and N_i is the concentration of the non-compensated ionized donors. The N_i is related to the slope of C^{-2} vs. V curve and can be obtained from the expression given below

$$N_i=\frac{2}{q\varepsilon_s\varepsilon_o A^2}\left[\frac{1}{d(C^{-2})/dV}\right]. \tag{23}$$

The BH deduced from capacitance is then obtained from

$$\Phi_b^C=V_{bi}+V_n+\frac{kT}{q}-\Delta\phi \tag{24}$$

where V_n, referred to as the Fermi level potential, is the energy difference between the Fermi level and the bottom of the conduction band, and given by $V_n=kT/q[\ln(N_c/N_i)]$. Thus, Eq. (24) can be rewritten by neglecting the image-force barrier lowering ($\Delta\phi$) as

$$\Phi_b^C=V_{bi}+\frac{kT}{q}\left[1+\ln\frac{N_c}{N_i}\right], \tag{25}$$

where N_c (=5.4 $\times$ 10^{17} cm^{-3}) is the effective density of states in the conduction band for n-InP at 300 K [21].

Fig. 9 shows the reverse bias $C^{-2}-V$ plots for the Au/MD n-InP SBD as a function of temperature for a modulation frequency of 1.0 MHz. The capacitance of the diode in the range of 0.0 to −1.0 Volts has increased with increasing temperature as can be seen from Fig. 9. On the contrary of Fig. 3 in [18] linear $C^{-2}-V$ plots were obtained for the whole investigated temperature range. This indicates a constant donor concentration in the depletion layer and absence of metal-semiconductor interaction. Furthermore, the linear behaviour of the curves can be explained by the fact that the interface states and the inversion layer charge can not follow the a.c. signal at 1.0 MHz and consequently do not contribute appreciably to the diode capacitance. The V_{bi} and N_i values are obtained from the intercepts and the slopes of the extrapolated C^{-2}–V lines with the V_r axis, respectively. Then, the values of Φ_b^C are calculated by using Eq. (25). The N_i values, ranged from 8.27×10^{15} to 9.05×10^{15} cm^{-3} for 60–300 K temperature interval, are in good agreement with the values given by manufacturer. The values for the BH deduced from the C–V data are also shown in Fig. 3 as closed diamonds. The temperature dependence of the Φ_b^C can be fitted with $\Phi_b^C=\Phi_b^C(T=0)+\alpha T$ [10]. Where, $\Phi_b^C(T=0)$ and α

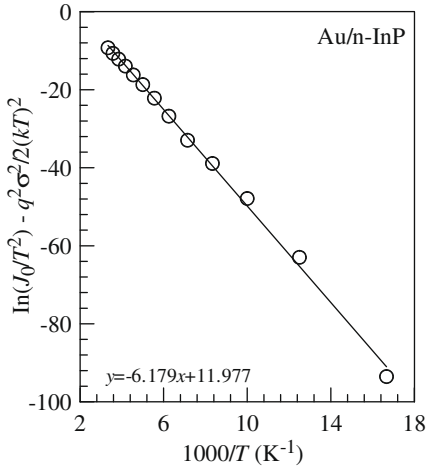

Fig. 8. Modified Richardson plot, $\ln(J_0/T^2)-(q^2\sigma_{s0}^2/2k^2T^2)$ vs. 1000/T, and its linear fit for the Au/MD n-InP Schottky diode according to Gaussian distribution of the barrier heights.

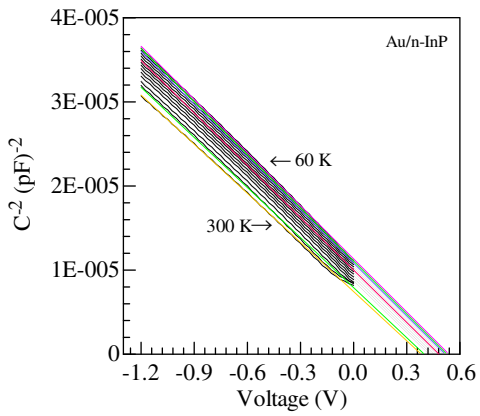

Fig. 9. The reverse bias C^{-2}–V characteristics of the Au/MD n-InP Schottky barrier diode at different temperature.

represent the barrier height extrapolated to the absolute zero and the temperature coefficient of the Φ_b^C, respectively. The fit of the Φ_b^C data with this expression shown in Fig. 3 gives $\alpha = -1.85 \times 10^{-4}$ eVK^{-1} and $\Phi_b^C(T=0) = 0.568$ eV. The value of α is in also close agreement with the -3.3×10^{-4} eVK^{-1} reported by Song et al. [26] for the Al/p-InP Schottky structure. Meanwhile, the value of α is in also close agreement with the value of the temperature coefficient of the band gap (-4×10^{-4} eVK^{-1}) for InP [49]. It can be concluded that the variation of the barrier height due to the temperature should follow almost the variation of the semiconductor band gap as the temperature coefficient of the Φ_b^C nearly equals to that of the band gap of InP.

From Fig. 3, the Φ_b^C values are seen to be higher than the Φ_{b0}^j values in the investigated temperature range. For the differences in BH values, some general reasons have been mentioned in the literature, such as surface contamination at the interface, deep impurity levels, an intervening insulating layer, quantum-mechanical tunnelling, image-force lowering and edge leakage currents [5,7,19]. There have also been some reports showing that the discrepancy between BHs measured by different techniques might be associated with the instrumentation problems; namely, the way to determine true space charge capacitance from *C–V* data or a large series resistance, which could affect the value determined from *I–V* data [5,50].

The discrepancy between Φ_{b0}^j and Φ_b^C as well as the strong temperature dependence of Φ_{b0}^j and n at low temperatures, can also be explained by assuming a Gaussian distribution of BHs with a mean value $\overline{\Phi}_{b0}^j$ and a standard deviation σ_{s0} [3,25,26,41–43]. Werner and Güttler [3] have algebraically confirmed that the current-barrier values (Φ_{b0}^j) are lower by a value which depends on the standard deviation σ_{s0}, whereas, the capacitance depends only on the mean band bending $\overline{\Phi}_{b0}^j$ and it is insensitive to the standard deviation σ_{s0} of the barrier height distribution $P(\Phi_{b0})$. Hence, the capacitance barrier Φ_b^C is equal to the mean barrier $\overline{\Phi}_{b0}^j$, i.e.:

$$\Phi_b^C \equiv \overline{\Phi}_{b0}^j. \tag{26}$$

Assuming a linear temperature dependence of σ_{s0}^2 as $\sigma_{s0}^2(T) = \sigma_{s0}^2(T=0) + \alpha_{\sigma_{s0}} T$, the Eqs. (19) and (26) should yield a relationship between Φ_{ap} and Φ_b^C as

$$\Phi_b^C - \Phi_{ap} = \frac{q\sigma_{s0}^2(T=0)}{2kT} + \frac{q\alpha_{\sigma_{s0}}}{2k}. \tag{27}$$

Fig. 10 shows the experimental $\Phi_b^C - \Phi_{ap}$ versus $1/2kT$ plot according to Eq. (27). This plot must give a straight line with a slope σ_{s0}^2 and an ordinate intercept $\alpha_{\sigma_{s0}}$. The slope and the ordinate intercept of the plot have given the values of $\sigma_{s0}(T=0) = 0.064$ eV and $\alpha_{\sigma_{s0}} = -1.9 \times 10^{-6}$ (eV)^{2}K^{-1}, respectively. The value of σ_{s0} in the investigated temperature region is in close agreement with the value of $\sigma_{s0} = 0.060$ eV from the plot of Φ_{ap} versus $1/2kT$ given in Fig. 7 which is not small when compared to the mean BH value of 0.532 eV. Hence, these significantly large potential fluctuations drastically affect low temperature *I–V* data and, in particular, they could be responsible for the curved behaviour of the conventional Richardson plots as in Fig. 4.

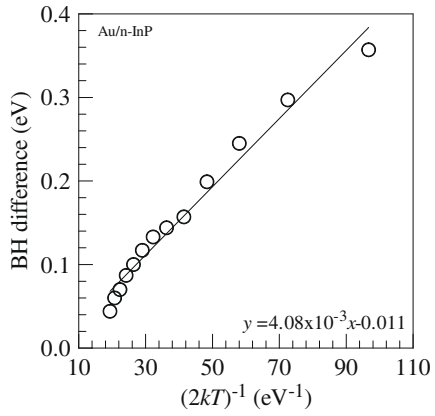

Fig. 10. Barrier height difference between values as derived from the conventional evaluation of *J–V* and *C–V* data as a function of inverse temperature.

4. Conclusion

The current transport mechanism in Au/MD n-InP SBDs has been investigated by means of *I–V* and *C–V* measurements at various temperatures between 60–300 K. It is found that the ideality factor n of the diode decreases while the corresponding zero-bias SBH increasing with an increase in temperature. The significant decrease of zero-bias BH and the increase of the ideality factor at low temperatures can not be caused by the processes such as tunnelling, generation-recombination currents, image-force lowering etc. Despite a linearity of $ln(J_{0f}/T^2)$ vs. $1000/nT$ Arrhenius plot for the flat-band saturation current density, it yields larger BH values than the zero-bias BH and unreasonably high effective (corrected) Richardson constant value being 0.622 eV and 25.34 Acm^{-2}K^{-2}, respectively. Also, the flat-band barrier height Φ_b^f is always larger than the zero-bias BH Φ_{b0}^j and it increases with decreasing temperature in the range of 300-100 K in a manner of the capacitance BH Φ_b^C. Therefore, the concept of flat-band barrier height is inadequate in removing the influence of inhomogeneities on the evaluation of *J–V* curves of the present Au/MD n-InP SBDs.

Abnormal behaviour in the temperature dependent ideality factor and the barrier height in the Au/MD n-InP SBDs have been successfully cleared up accounting the *TE* theory with a Gaussian distribution of the BH having spatial variations. The laterally homogeneous SBH and its standard deviation are of 0.526 eV and 0.060 eV, respectively. Also, the mean barrier height and the Richardson constant values have been obtained as 0.532 eV and 15.9 Acm^{-2}K^{-2}, respectively, by means of the modified Richardson plot, $\ln(J_0/T^2) - (q^2\sigma_{s0}^2/2k^2T^2)$ vs. $1000/T$. This value of Richardson constant is in close agreement with the theoretical value of 9.4 AK^{-2}cm^{-2} of electrons in n-type InP. However, the interpretation of the discrepancy between the Φ_{b0}^j and Φ_b^C by Gaussian distribution of BHs leads to more meaningful results and *TE* theory with a Gaussian distribution of SBHs is thought to be responsible for the electrical behaviour of the whole investigated temperature range. In conclusion, it can be speculated from the diode parameters obtained by *I–V* and *C–V* techniques that the spatial inhomogeneities of the SBHs is an important factor and could not be ignored in the analysis of temperature dependent electrical characterization of the Schottky structures.

Acknowledgement

The authors wish to thanks to Dr. H S Güder for his helpful critical reading of the manuscript.

References

[1] M.K. Hudait, K.P. Venkateswarlu, S.B. Krupanidhi, Solid-State Electron. 45 (2001) 133;
M.K. Hudait, S.B. Krupanidhi, Phys. B 307 (2001) 125.
[2] S. Chand, J. Kumar, J. Appl. Phys. 80 (1) (1996) 288.
[3] J.H. Werner, H. H Güttler, J. Appl. Phys. 69 (1991) 1522.
[4] C.T. Chuang, Solid-State Electron. 27 (1984) 299.
[5] R.T. Tung, Phys. Rev B. 45 (1992) 13502;
R.T. Tung, Mater. Sci. Eng. R. 35 (2001) 1–138.
[6] F. A Padovani, in: R.K. Willardson, A.C. Beer (Eds.), Semiconductor and Semimetals, vol. 7A, Academic Press, New York, 1971.
[7] C.R. Crowell, Solid-State Electron. 20 (1977) 171.

[8] R.T. Tung, J.P. Sullivan, F. Schrey, Mater. Sci. Eng. B 14 (1992) 266.
[9] R.F. Schmitsdrof, T.U. Kampen, W. Mönch, J. Vac. Technol. B 15 (1997) 1221.
[10] S.Y. Zhu, R.L. Van Meirhaeghe, C. Detavernier, F. Cordan, G.P. Ru, X.P. Qu, B.Z. Li, Solid-State Electron. 44 (2000) 663.
[11] H. Wen-Chang, L. Tan-Fu, L. Chung-Len, J. Appl. Phys. 78 (1995) 1.
[12] Zs.J. Horváth, V. Rakovics, B. Szentpáli, S. Püspöki, Phys. Stat. Sol. C (2003) 916.
[13] P.G. McCafferty, A. Sellai, P. Dawson, H. Elabd, Solid-State Electron. 39 (1996) 583.
[14] N. Newman, T. Kendelwicz, L. Bowman, W.E. Spicer, Appl. Phys. Lett. 46 (1985) 1176.
[15] Zs.J. Horváth, V. Rakovics, B. Szentpáli, S. Püspöki, K. Žyďánskŷ, Vacuum 71 (2003) 113.
[16] L.J. Brillson, C.F. Brucker, A.D. Katnani, N.G. Stoffel, G. Margaritondo, Appl. Phys. Lett. 38 (1981) 784.
[17] E. Hökelek, G.Y. Robinson, J. Appl. Phys. 54 (1983) 5199.
[18] H. Çetin, E. Ayyildiz, Semicond. Sci. Technol. 20 (2005) 625.
[19] S.M. Sze, Physics of Semiconductor Device, second ed., Wiley, New York, 1981. p. 245.
[20] E.H. Rhoderick, R.H. Williams, Metal–Semiconductor Contacts, second ed., Clarendon, Oxford, 1988.
[21] A. Neamen Donald, Semiconductor Physics and Devices, Irwin, Boston, 1992; C.W. Wilmsen, Physics and Chemistry of III–V Compound Semiconductor Interface, Plenum, New York, 1985.
[22] N. Szydlo, J. Oliver, J Appl. Phys. 50 (1979) 1445.
[23] Z. Benamara, B. Akkal, A. Talbi, B. Gruzza, L. Bideux, Mater. Sci. Eng. C 21 (2002) 287.
[24] Z.Q. Shi, R. Wallace, W.A. Anderson, Appl. Phys. Lett. 59 (1991) 446.
[25] J.H. Werner, H.H. Güttler, J. Appl. Phys. 73 (1993) 1315.
[26] Y.P. Song, R.L. Van Meirhaeghe, W.H. Laflare, F. Cardon, Solid-State Electron. 29 (1986) 633.
[27] A. Gümüş, A. Türüt, N. Yalçın, J. Appl. Phys. 91 (2002) 1 245.
[28] S. Chand, J. Kumar, J. Appl. Phys. 80 (1996) 288.
[29] S. Zhu, C. Detavernier, R.L. Van Meirhaeghe, F. Cardon, G.P. Ru, X.P. Qu, B.Z. Li, Solid-State Electron. 44 (2000) 1807.
[30] S. Bandyopadhyay, A. Bhattacharyya, S.K. Sen, J. Appl. Phys. 85 (1999) 3671.
[31] F.E. Jones, B.P. Wood, J.A. Myers, C.D. Hafer, M.C. Lonergan, J. Appl. Phys. 86 (1999) 6431.
[32] N. Newman, M.V. Schilfgaarde, T. Kendelwicz, M.D. Williams, W.E. Spicer, Phys. Rev. B 33 (1986) 1146.
[33] M. Wittemar, Phys. Rev. B 42 (1990) 5249.
[34] S. Asubay, Ö. Güllü, B. Abay, A. Türüt, A. Yilmaz, Semicond. Sci. Technol. 23 (2008) 035006.
[35] Zs. J. Horváth, Solid-State Electron. 39 (1996) 176.
[36] L.F. Wagner, R.W. Young, A. Sugerman, IEEE Electron Dev. Lett. EDL-4 (1983) 320.
[37] H.H. Güttler, J.H. Werner, Appl. Phys.Lett. 56 (1990) 1113.
[38] M.H. Unewisse, J.W.V. Storey, J. Appl. Phys. 73 (1993) 3873.
[39] M. Missous, E.H. Rhoderick, J. Appl. Phys. 69 (1991) 7142.
[40] S. Zhu, R.L. Van Meirhaeghe, S. Forment, G.P. Ru, X.P. Qu, B.Z. Li, Solid-State Electron. 48 (2004) 1205.
[41] J.P. Sullivan, R.T. Tung, M.R. Pinto, W.R. Graham, J Appl. Phys. 70 (1991) 7403.
[42] Y.G. Chen, M. Ogura, H. Okushi, Appl. Phys. Lett. 82 (2003) 4367.
[43] H.K. Henisch, Semiconductor Contacts, Oxford University, London, 1984. p. 123.
[44] R.F. Schmitsdorf, T.U. Kampen, W. Mönch, Surf. Sci. 324 (1997) 249.
[45] S. Anand, S.B. Carlsson, K. Deppert, L. Montelius, L. Samuelson, J. Vac. Sci. Technol. B 14 (1996) 2794.
[46] E. Dobročka, J. Osvald, Appl. Phys. Lett. 65 (1994) 575.
[47] A. Ashok Kumar, V. Janardhanam, V. Rajagopal Reddy, P. Narasimha Reddy, J. Optoelectron. Adv. Mater. 9 (2007) 3877.
[48] A. Van der Ziel, Solid State Physical Electronics, second ed., Prentice-Hall, Englewood Cliffs, NJ, 1968.
[49] Y.F. Tsay, B. Gong, S.S. Mitra, Phys. Rev. B 6 (1972) 2330.
[50] W. Mönch, Appl. Phys. Lett. 72 (1998) 1899.